J Comput Neurosci () :
DOI 10.1007/s10827-006-4791-8

An intracellular Ca^{2+} subsystem as a biologically plausible source of intrinsic conditional bistability in a network model of working memory

Christopher P. Fall · John Rinzel

Received: 18 March 2005 / Revised: 26 August 2005 / Accepted: 2 September 2005 / Published online: 20 February 2006

Abstract We have developed a firing rate network model for working memory that combines Mexican-hat-like synaptic coupling with intrinsic or cellular dynamics that are conditionally bistable. While our approach is in the spirit of Camperi and Wang (1998) we include a specific and plausible mechanism for the cellular bistability. Modulatory neurotransmitters are known to activate second messenger signaling systems, and our model includes an intracellular Ca^{2+} handling subsystem whose dynamics depend upon the level of the second messenger inositol 1,4,5 trisphosphate (IP3). This Ca^{2+} subsystem endows individual units with conditional intrinsic bistability for a range of IP3. The full "hybrid" network sustains IP3-dependent persistent ("bump") activity in response to a brief transient stimulus. The bump response in our hybrid model, like that of Camperi-Wang, is resistant to noise – its position does not drift with time.

Keywords persistent activity · working memory · computational model · calcium signaling · inositol 1,4,5 trisphosphate · neuromodulators

1. Introduction

There is great interest in how the brain can maintain the persistent neural activity encoding recent stimuli that is thought to be the basis of working memory (Fuster, 1988). Several theoretical mechanisms for the maintenance of persistent activity have been described (Durstewitz et al., 2000), including local recurrent feedback and intrinsic persistent activity on a single-cell basis. Recurrent excitation at the local circuit level has received the most attention, from Hopfield models through elaborated conductance unit networks (Durstewitz et al., 2000; Wang, 2001).

Wilson and Cowan suggested that meaningful insight into the behavior of neural ensembles might be gained by a mean field approach describing the average rate of firing over some coherent population (Wilson and Cowan, 1972). Averaging on a local scale in combination with lateral connectivity described by a spatial kernel with wider support leads to a continuum, integrodifferential description of spatiotemporal neural activity (Wilson and Cowan, 1973). At the same time, there is now renewed interest in the concept that individual neurons might have some inherent ability to sustain persistent activity without recurrence. The remarkable finding that individual entorhinal cortical neurons can sustain graded persistent activity (Egorov et al., 2002) is the perhaps most striking example to date.

At the intersection of these ideas is a model by Camperi and Wang (C-W) which explores the idea of bistability in individual neurons within an Amari-type (Amari, 1977) integrodifferential network model (Camperi and Wang, 1998). Camperi and Wang simulate working memory for head position using a ring of individual cells, each with ad-hoc intrinsic conditionally bistable dynamics, which are connected by a lateral inhibition, "Mexican hat"-like weight kernel that spans the spatial domain. This conditional bistability requires network activity to move individual cells into a range of activity where they can access a range of bistability in the firing rate function. The time course of a working memory bump in response to a transient stimulus for the C-W model is shown

Action Editor: Upinder Bhalla

C. P. Fall (✉)
Department of Anatomy and Cell Biology, University of Illinois at Chicago Medical Center,
808 South Wood St., Room 578, M/C 512, Chicago, IL 60612
e-mail: fall@uic.edu

J. Rinzel
New York University, Center for Neural Science and Courant Institute of Mathematical Sciences,

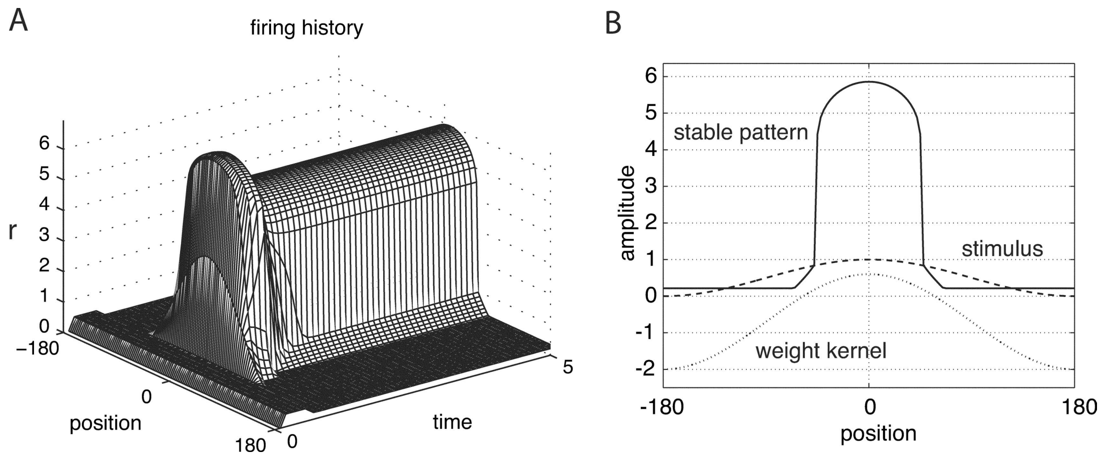

Fig. 1 **(A)** The C-W model responds to a sufficient stimulus by "remembering" the location with a bump of activity. This bump is translation invariant. **(B)** The shape of the steady state bump for the C-W model under standard parameters is shown in solid. The typical stimulus for all simulations in this manuscript is shown dashed. The weight kernel for all simulations in this manuscript except for the C-W non-bistable case (Fig. 6B; $W_I = 1$ and $W_E = 2.9$) is shown dashed.

in Fig. 1A. The shape of the final pattern, together with the shape of the weight kernel and the stimulus used in these simulations is shown in Fig. 1B.

The biological basis for such bistability remains little explored. Ca^{2+} has been shown experimentally (Egorov et al., 2002) and theoretically (Fransen et al., 2002) to contribute to persistent firing of neurons, via upregulation of a nonspecific cation current. Neuromodulators linked to Ca^{2+} release or Ca^{2+} sensitive signaling cascades have been shown to increase synaptic NMDA currents (Seamans et al., 2001) and the persistent sodium current (Yang and Seamans, 1996), both of which might increase the efficacy of synaptic input. There is a fair amount of controversy over the effects of neuromodulators (Seamans and Yang, 2004), and here we consider only the possibility that neuromodulators increase neuronal excitability or input efficacy.

Theoretical analyses suggest that regenerative intracellular Ca^{2+} release might play a role in intrinsic bistability of single neurons (Loewenstein and Sompolinsky, 2003; Teramae and Fukai, 2005). Dendrites of cortical neurons contain intracellular Ca^{2+} release machinery which is activated by neuromodulators and which affects neuronal integration (Nakamura et al., 1999, 2000; Barbara, 2002). Indeed, cortical pyramidal cells support IP3-mediated Ca^{2+} waves resulting from afferent stimulation (Larkum et al., 2003). Here we explore a hybrid model of working memory which replaces the cubic firing rate function in C-W with an intracellular Ca^{2+} subsystem for generating the intrinsic conditional bistability (De Young and Keizer, 1992; Atri et al., 1993; Li and Rinzel, 1994). A cartoon of this system is shown in Fig. 2A. We treat the level of the second messenger IP3 as a proxy for the signaling cascade initiated by neuromodulators like dopamine and acetylcholine. The Ca^{2+} subsystem is tunable through different dynamic regimes. As the level of IP3 increases it shows transitions from a monostable steady state (low Ca^{2+}) to bistability to a monostable high Ca^{2+} state. The network-driven activity and cellular subsystem interact synergistically, such that Ca^{2+} increases the efficacy of synaptic input, and synaptic input increases cytosolic Ca^{2+}. The network is able to sustain IP3-dependent persistent ("bump") activity in response to a stimulus, and it is resistant to noise.

2. The Model

The integrodifferential structure of the network model's synaptic interactions, with a lateral inhibition kernel and a ring topology, are like those in the C-W model (Camperi and Wang, 1998). The model's units can be viewed as individual neurons or as groupings from discretization with local averaging to represent near-identical behavior of nearby neurons (nearby in physical or feature space). In C-W intrinsic bistability was induced with a cubic firing rate function *f(r)* and formulated such that a region of stable low firing states and stable high firing states co-exist. We have replaced this ad-hoc intrinsic bistability in the C-W model with a Ca^{2+} release subsystem. In our hybrid formulation, intracellular Ca^{2+} concentration (Ca) can be thought to facilitate postsynaptic neuronal input, which in turn contributes to Ca via a plasma membrane Ca^{2+} flux through synaptic and voltage gated channels in the dendrites. Our model has 3 dynamic variables, not just one as in C-W.

The equation describing the firing activity of each neuron is given by

$$\tau_r \frac{dr}{dt} = -f(r) + g(I)(1 + Ca). \tag{1}$$

The nondimensional firing rate is a balance between the firing rate function, *f*(*r*), and the background and synaptic

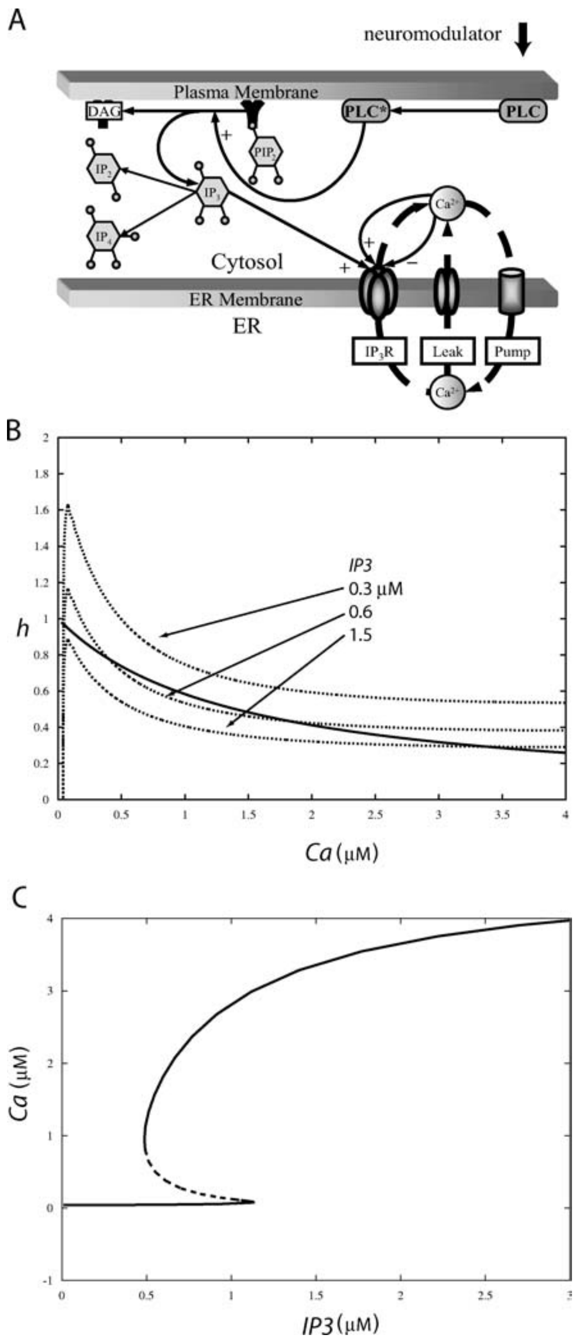

Fig. 2 **(A)** IP3 liberated as a result of modulatory transmitter action binds to the intracellular Ca^{2+} release channel in the endoplasmic reticulum. IP3 serves as a "permissive switch" for autocatalytic Ca^{2+} release through this Ca^{2+} sensitive Ca^{2+} channel. (B) The Ca^{2+} subsystem alone (Eqs. (2–3) with $J_{\text{syn}} = 0$). Shown are *Ca* (dashed) and *h* (solid) nullclines for $IP3 = 0.3\ \mu$M, 0.6 μM and 1.5 μM. As *IP3* is increased, the Ca^{2+} subsystem progresses from one stable low *Ca* state through bistability to one stable high *Ca* state. (C) Bifurcation diagram for the Ca^{2+} subsystem alone with *IP3* as a parameter. The region of bistability is from $IP3 = 0.48\ \mu$M to IP3 $= 1.14\ \mu$M.

input given by $g(I)$. We retain nondimensionality in the firing rate for familiarity with C-W but the Ca^{2+} subsystem that follows below has physical units: *IP3* and *Ca* are both expressed in μM. A key ingredient for getting stabilized bump activity in the C-W model is the nonlinear function of the firing rate, $f(r) = c + r - ar^2 + br^3$, which was tuned to be cubic in shape and could thereby lead to intrinsic bistability over a range of input values. In contrast, we choose the firing function to be monotonic; it is *not* N-shaped in order to create intrinsic bistability. With other parameter changes, our model is capable of generating bumps even with a linear $f(r)$ of slope 1, however the firing rates are not comparable to C-W and we do not report these results here. In our model, Ca^{2+} increases the efficacy of synaptic input via coupling to the *Ca* state variable.

The synaptic input to a neuron consists of recurrent input (given by the convolution over the weights and firing rates of other neuron) plus synaptic input from extrinsic neuronal sources:
$I(\theta_i, t) = I_{\text{ext}}(\theta_i, t) + \sum_{j=1}^{n} \frac{1}{N} W(\theta_i - \theta_j) r(\theta_j, t)$, and the total synaptic input, I, is thresholded so that $g(I) = I : I > 0$ and $g(I) = 0 : I \leq 0$. For simulations with noise, uniform white noise is added to I.

As in C-W, the connectivity weight kernel has a lateral inhibition form which is given by $W(\theta) = -W_I + W_E(\frac{1+\cos(\theta)}{2})^q$. This is analogous to a "Mexican hat" function, however these functions typically decay to zero such that the influence of neurons (excitatory or inhibitory) does not extend over the whole spatial domain. In this case, with a shifted cosine function, the network is essentially fully connected because this weight function only has zero value at 2 places on the ring.

The external input with constant (I_o) and transient (I_{cue}) components, is also given by a shifted cosine:

$$I_{\text{ext}}(\theta, t) = I_o + H(t_{\text{off}} - t) \cdot I_{\text{cue}} \left(\frac{1 + \cos(\theta)}{2} \right)^p,$$

where H is the Heaviside function and the stimulus is usually presented for 0.5 s. θ is the phase difference between neurons in the weight kernel and in the stimulus shape calculations. The shapes of these curves can be seen in Fig. 1B for standard parameters.

The Ca^{2+} subsystem (Fig. 2A) operates via IP3-modulated Ca^{2+}-induced Ca^{2+}-release from the internal endoplasmic reticulum store with concentration Ca_{ER}. In this early model, we specify Ca_{ER} as constant. The key property for this system is positive feedback of *Ca* onto the IP3 sensitive Ca^{2+} channel (known as the IP3 receptor or IP3R), and then a slow IP3R inactivation which also depends on *Ca*. SERCA calcium pumps have a nonlinear dependence on *Ca* and remove Ca^{2+} from the cytosol. For the integrated model here, we assume a pump term which combines plasma membrane and ER SERCA pumps. The interplay of Ca-dependent rates of release and reuptake by these players results in a rich repertoire of dynamical behavior (De Young and Keizer, 1992). A balance equation describes the evolution of Ca, including release of Ca^{2+} through the IP3R into the cytosol (J_{IP3R}), removal of Ca^{2+} from the cytosol (J_{SERPM}) and a leak flux from the ER to the cytosol (J_{Leak}). Importantly, this equation contains J_{syn}, which is the *external* contribution to Ca^{2+} influx from synaptic activity.

$$\frac{dCa}{dt} = (J_{\mathrm{IP3R}} - J_{\mathrm{SERPM}} + J_{\mathrm{Leak}} + J_{\mathrm{syn}}) \quad \text{where } J_{\mathrm{syn}} = g(I) \tag{2}$$

The terms that couple Eqs. (1) and (2) are not identical; if they were the rightmost term in (2) would be $g(I)(1+\alpha Ca)$. We found that such symmetrical coupling, with additional positive feedback to the Ca dynamics, led to oversensitivity to parameter variations in the model. It is not unreasonable to invoke asymmetry: In our idealized model we do not distinguish which synaptic currents carry Ca^{2+}, and we assume that some unspecified fraction of the synaptic current involves Ca^{2+}-influx—such as through the NMDA receptor. Voltage-gated Ca^{2+} channels, local to synapses or associated dendrite, would also be activated by postsynaptic depolarization. We also assume that some portion of the synaptic current that influences post-synaptic spiking is facilitated by Ca^{2+} but does not carry Ca^{2+}. In this case we envision Ca^{2+} -mediated second messenger pathways which might phosphorylate ion channels such as the NMDA and AMPA receptors.

The parameters for the Ca^{2+}-balance Eq. (2) assume a rapid buffer approximation (De Young and Keizer, 1992). The rates are based on those in (Fall et al., 2004), however here all scale factors for compartment size and buffering are incorporated into the parameter values such that the units are in terms of concentration per time. In this formulation we do not use an explicit endoplasmic reticulum (ER Ca^{2+} is fixed) and Ca^{2+} is not conserved as in (De Young and Keizer, 1992).

The time scale of the Ca^{2+} subsystem is controlled by the slow gating variable h that represents the proportion of IP3R's not inactivated by Ca:

$$\frac{dh}{dt} = \frac{h_\infty - h}{\tau_h}, \quad \text{where} \quad h_\infty = \frac{k_{\mathrm{inh}}}{k_{\mathrm{inh}} + Ca}. \tag{3}$$

Several auxiliary expressions complete the Hodgkin-Huxley like formalism which describes the Ca-dependent fluxes outlined above, including fast activation of the IP3R's via the gating relation m_∞:

$$J_{\mathrm{IP3R}} = v_{\mathrm{IP3R}} m_\infty^3 h^3 (Ca_{\mathrm{ER}} - Ca), \quad \text{where}$$

$$m_\infty = \frac{IP3}{IP3 + k_{\mathrm{IP3}}} \frac{Ca}{Ca + k_{\mathrm{act}}},$$

$$J_{\mathrm{Leak}} = v_{\mathrm{Leak}}(Ca_{\mathrm{ER}} - Ca),$$

and $J_{\mathrm{SERPM}} = v_{\mathrm{SERPM}} \dfrac{Ca^2}{k_{\mathrm{SERPM}}^2 + Ca^2}$.

Equations (2)–(3), along with the auxiliary relationships above, constitute the Ca^{2+} subsystem. Here we have considered only fixed IP3 as a simplification. IP3 is certainly dynamic, its production may also be Ca^{2+} sensitive, and such a system has been modeled in other cells (Fall et al., 2004; Wagner et al., 2004).

The parameters are described in Table 1. Explorations of the model were conducted using custom code written in MATLAB (R14) and simulated on an Apple Macintosh G5 computer. This code is available upon request from the authors. A forward Euler integration scheme was used with a time step of 0.001s; a smaller time step did not affect the results. 128 neurons were simulated in the data presented here. XPPaut was used to compute dynamical characteristics (phase plane properties) of the Ca^{2+} subsystem (Ermentrount, 2002). For stochastic simulations, 128 neurons were simulated and uniformly distributed noise of amplitude 1.5 centered around 0 (−0.75, 0.75) was added to the input (I). Replications were performed by reseeding the matlab "rand" function 1000 times. Each model was evaluated using the same sequence of seeds and thus the same noise input to I.

3. Results

3.1. A Bistable Ca^{2+} Subsystem Supports Bump Patterns

Standing alone, uncoupled from the firing dynamics, the DeYoung-Keizer IP3-mediated Ca^{2+} release model can be tuned for different dynamical behaviors using the level of the second messenger IP3 as a control parameter (De Young and Keizer, 1992; Li and Rinzel, 1994). In some parameter regimes (Fall et al., 2004), increasing *IP3* causes the Ca^{2+} model to pass from a single stable steady state at a lower level of Ca through a region of bistability and then on to one stable elevated state. In the intermediate bistable regime, low and high stable Ca^{2+} levels are possible, and a perturbation from the low Ca^{2+} state of sufficient amplitude (dependent on *IP3*) pushes the system into the high Ca^{2+} state. Figure 2B shows the nullclines of the Ca^{2+} subsystem (where derivatives of the state variables Ca and h are zero) for several values of the parameter IP3. The Ca nullcline for $IP3 = 0.6\ \mu$M intersects the h nullcline three times; the central intersection is unstable. This results in a system that can exist in either the high or low Ca state. A bifurcation curve showing the stable (solid) and unstable (dashed) fixed points for the system and the range of bistability is given in Fig. 2C.

Table 1. Model parameters unless otherwise indicated. Rates for the Ca^{2+} subsystem are in terms of μM/s, concentrations in μM and time in s.

C-W model			Ca^{2+} subsystem		
Symbol	Parameter	Value	Symbol	Parameter	Value
τ_r	Integration time constant	0.025 s	Ca_{ER}	ER Ca^{2+}concentration	11
p	Stimulus shape exp	1	τ_h	IP3R inact. time const	0.5
q	Weight shape exponent	1	$vIP3$	IP3R Ca^{2+} flux	80
I_o	Background activity	0.35	$vLeak$	Ca^{2+} leak flux	0.00032
I_{cue}	Stimulus amplitude	1	v_{SERPM}	Ca^{2+} pump flux	3.33
a	Nonlinearity parameter	0.3	k_{SERPM}	Ca^{2+} pump *sensitivity*	0.4
b	Nonlinearity parameter	0.033	k_{IP3}	IP3R IP3 sens	0.4
c	Nonlinearity parameter	−0.3	k_{inh}	IP3R Ca^{2+} inhibition	1.4
W_I	Inhibitory strength	2	k_{act}	IP3R Ca^{2+} activation	1.1
W_E	Excitatory strength	2.6			

Such a bistable intracellular signaling system could be the basis for intrinsic bistability for neurons in a network. Our network framework is like that of the C-W model but we have replaced the ad hoc mechanism for bistability of an N-shaped firing rate function by a plausible intracellular Ca^{2+} subsystem. In our simulations we have modified the original C-W network model for firing dynamics that so that the firing rate function *f(r)* is no longer N-shaped and bistable, but instead is monotonic. While this monotonic firing rate function is still steep, under this condition the C-W model alone no longer supports working-memory like behavior unless other parameters such as the connectivity weights and background activity are changed (Camperi and Wang, 1998). A transient stimulus of any strength results in a network which returns to a baseline, uniform activity level.

We coupled this monostable C-W model to our intracellular Ca^{2+} release system such that, in each individual neuron, the firing activity contributes to the intracellular Ca^{2+} and intracellular Ca^{2+} increases the efficacy of synaptic input to the neuron. The Ca^{2+} subsystem is able to contribute sufficient bistability such that the hybrid model can sustain bump-like working memory patterns. These bumps are dependent on the level of the second messenger IP3. As shown in Fig. 3(A–B), when *IP3* is elevated to the point where the Ca^{2+} subsystem is bistable (here $IP3 = 0.6$ μM), such as might be the case due to neuromodulator receptor activation, the model is able to sustain the bump pattern of activity in response to the presented stimulus. A low level of *IP3* corresponding to a single low stable state in the Ca^{2+} subsystem results in no sustained firing pattern as seen in Fig. 3(C–D). When the Ca^{2+} release system was tuned for bistability ($IP3 = 0.6$ μM), bumps were readily evoked.

3.2. Excitable Subsystem Also Supports Bumps Through *Conditional* Bistability

Is *bistability* in the Ca^{2+} subsystem necessary for persistent neuronal firing? Should the Ca^{2+} subsystem have access to the high- Ca^{2+} state in the absence of elevated neuronal firing? While there are no reports of bistable Ca^{2+} release processes in neurons, there is evidence for the nonlinear amplification of backpropagating Ca^{2+} waves by IP3 sensitive intracellular Ca^{2+} release in dissociated cells (Barbara, 2002). Such amplification is the hallmark of an excitable system, wherein suprathreshold triggering of the dynamical system results in a large transient with eventual return to a single stable state.

C-W implemented *conditional* bistability in the firing rate function. That is, sufficient network activity was required in order for the firing rate function to be in the bistable regime. Similarly, we are able to build conditional bistability into our model neurons by tuning the DeYoung-Keizer Ca^{2+} subsystem into a regime where it is, when isolated, *excitable*. By reducing *IP3* from the bistable level $IP3 = 0.6$ μM, we can cause nonlinear amplification of the Ca^{2+} subsystem, however the only stable state of the subsystem *alone*, uncoupled from the firing rate dynamics, is the low Ca^{2+} state. This is shown in Fig. 4A, where the Ca^{2+} subsystem alone is perturbed with a small amplitude brief Ca^{2+} pulse. For *IP3* levels less than 0.2, there is no apparent amplification. For intermediate values of *IP3* (e.g. $IP3 = 0.4$ μM), the Ca^{2+} subsystem demonstrates excitability, and a small transient perturbation leads to a larger amplification and eventual return to rest. Beyond $IP3 = 0.4$, the excitable amplification grows until the system reaches bistability.

Even when the Ca^{2+} subsystem standing alone ($J_{\mathrm{syn}} = 0$) is tuned to excitability ($IP3 = 0.475$ μM), the hybrid network model is capable of sustaining bumps because the flux of Ca^{2+} entering through J_{syn} pushes the Ca^{2+} subsystem into bistability. The region in parameter space for excitability is very close to the regimes where the Ca^{2+} subsystem is bistable or monostable at high Ca^{2+} levels. As shown in Fig. 4B for the Ca^{2+} subsystem alone, steady Ca^{2+}-influx (here 1 μM/s), such as would enter via J_{syn} in the coupled system, shifts the Ca^{2+}-nullcline and changes its shape. Such input moves the Ca^{2+} subsystem to the bistable or monostable-high Ca^{2+} (depending on the coupling and other parameters). The condition shown in Fig. 4B for the Ca^{2+}

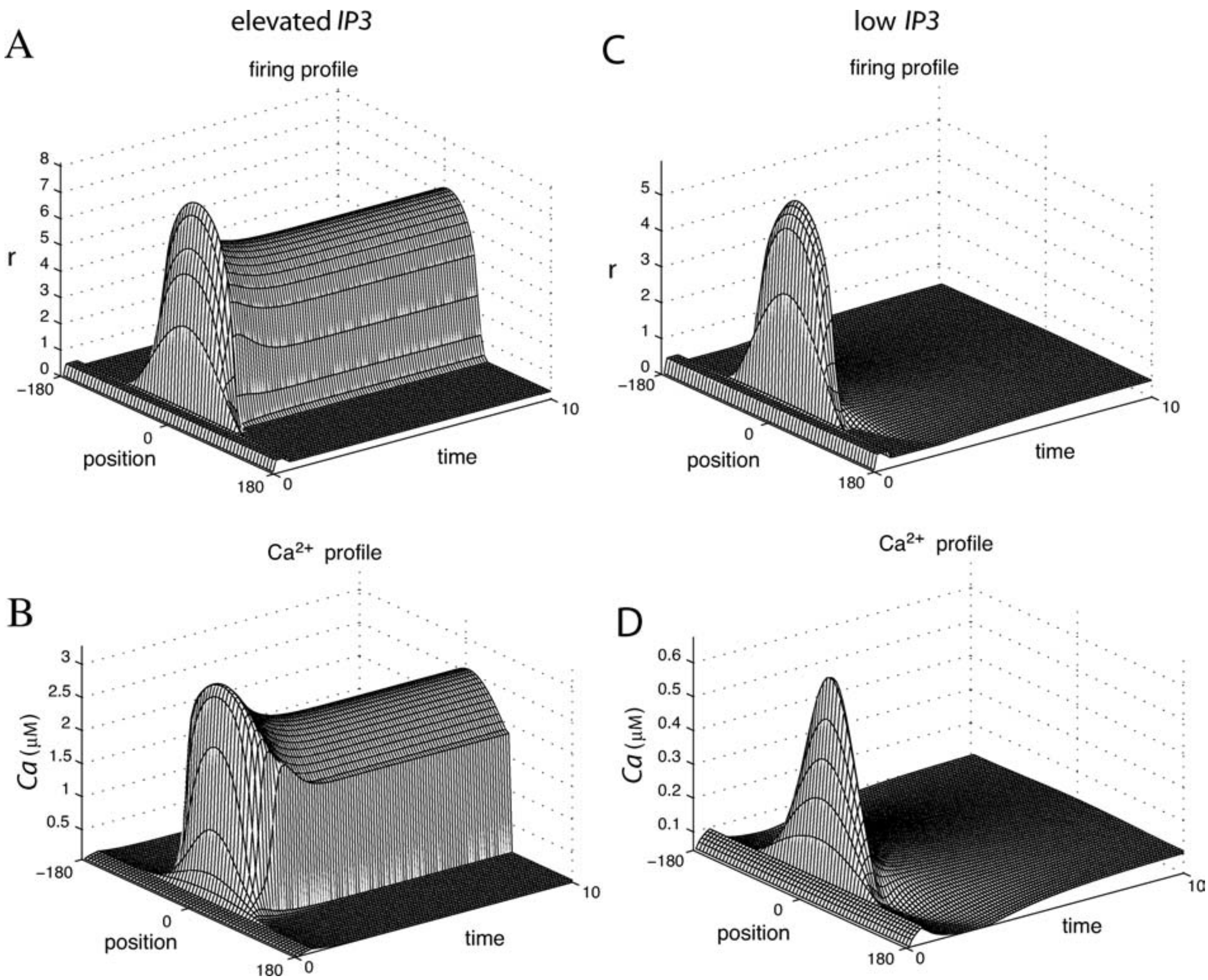

Fig. 3 Firing history and *Ca* history for low and elevated *IP3*. **(A)** firing history for *IP3* $= 0.3\ \mu$M (no persistent activity). **(B)** *Ca* for same condition as (A). **(C)** firing history for *IP3* $= 0.6\ \mu$M, showing persistent activity. **D:** *Ca* for same condition as (C).

subsystem alone is approximately the same as a neuron firing at the peak of a bump in the coupled hybrid system: the peak of the convolved input, $g(I)$, during a bump in the coupled system is on the order of 16% of the peak firing level (r) for the network under standard parameters (see also Fig. 5). So a neuron firing at a rate of 6 would see approximately an additional 1 μM/s of Ca^{2+} due to J_{syn}.

As there is a range of firing rates in a bump state, there will be a range of levels of external Ca^{2+} input via J_{syn}. Figure 4C shows the steady state for the Ca^{2+} subsystem alone over a range of J_{syn} (here a parameter) for several values of IP3. These curves demonstrate that external Ca^{2+} flux through J_{syn} has the effect of making bistability and monostable-high Ca^{2+} levels in the coupled system available at lower levels of *IP3* than would be the case without Ca^{2+} flux through J_{syn} (recall Fig. 2C for no J_{syn}). The thin dashed vertical line in Fig. 4C indicates the approximate level of J_{syn} (equal to g (I) for $\beta = 1$) that is seen by the first neuron within the bump, i.e. with a noticeably elevated steady state Ca^{2+} level (look ahead to Fig. 5C). This represents the transition point for the Ca^{2+} subsystem, and because external Ca^{2+} flux via J_{syn} occurs only in active neurons, the coupled hybrid system is conditionally bistable.

The range of *IP3* for which a transient stimulus results in a bump state is shown as a solid line in Fig. 4D. The uniform and stable state of the network for no transient stimulus is shown on the same figure in dots. Vertical dashed lines show the upper and lower bounds of bistability for the Ca^{2+} subsystem alone (see Fig. 2C). There is a range of low *IP3* levels for which no bump states can occur in the coupled hybrid model. In an adjacent region of *IP3* concentration, including the part of the region for which the Ca^{2+} subsystem alone is excitable and part of the region for which the Ca^{2+} subsystem alone is bistable, bumps in the coupled system can occur with stimulation and yet the low firing, uniform state is also stable. This corresponds to the range of working memory like behavior. Beyond this region, there is only a globally attracting bump state, and thus no network bistability. The effect of the influx of external Ca^{2+} due to synaptic activity is to shift (to smaller levels of IP3) and shrink the region of bistability for

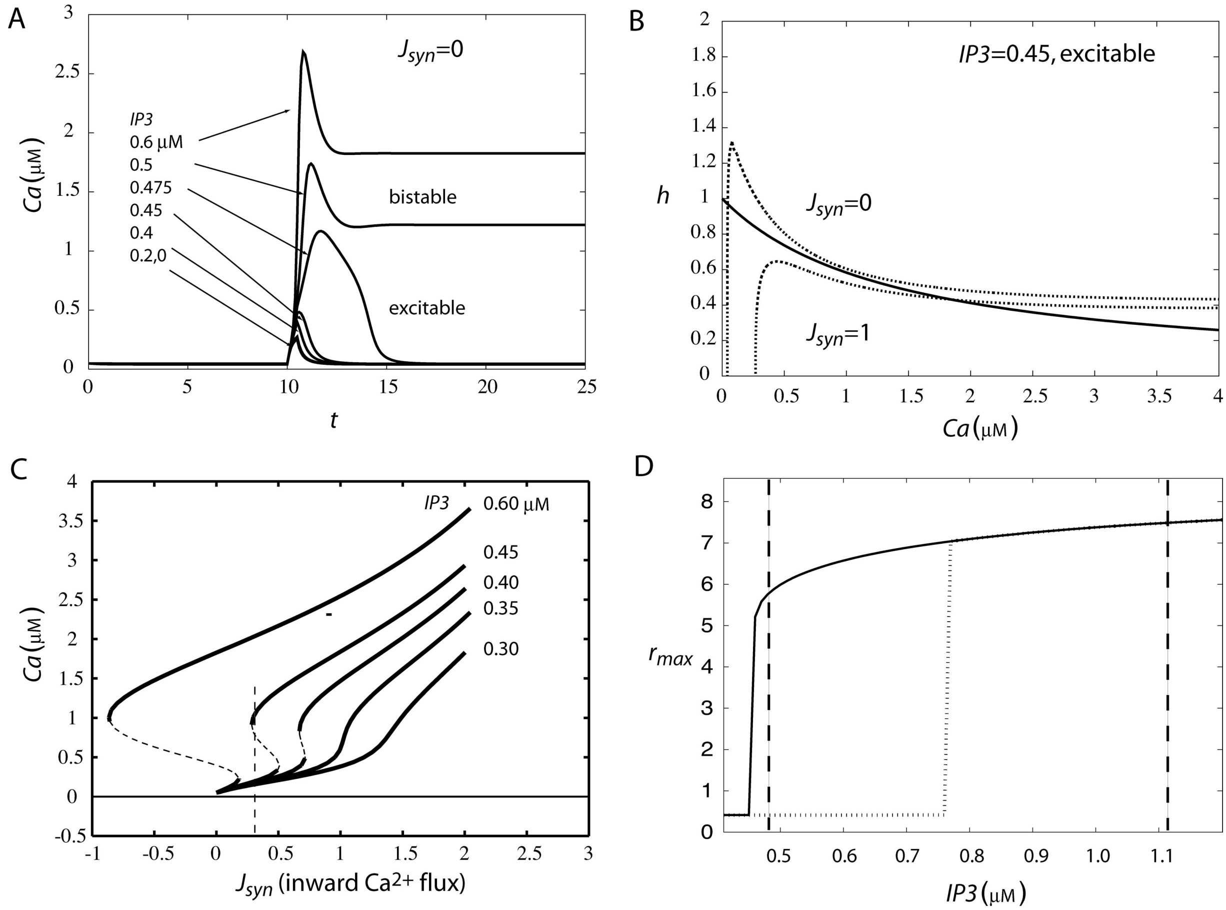

Fig. 4 **(A):** Excitable Ca^{2+} subsystem results in amplification of a small pulse (amplitude 1 μM/s, duration 0.5 s). Amplification increases with *IP3*. **(B):** External Ca^{2+} entering as a result of neuronal activity (considered here by treating J_{syn} as a parameter) shifts the Ca^{2+} null-cline. Curve shown results from 1 μM/s constant influx, which is of the same order as what would occur during maximum neuronal firing for the simulations reported here. **(C)** Bifurcation curves showing the stable (solid lines) and unstable (dashed portions) steady states for the Ca^{2+} subsystem as a function of constant external Ca^{2+} flux via J_{syn} for several values of *IP3*. Note that, in our hybrid model, J_{syn} does not go negative. The thin dashed vertical line indicates the approximate level of J_{syn} (equal to $g(I)$) that is seen by the first neuron within the bump. **(D)** Range of *IP3* for which network bumps result from transient stimulation (solid) and (uniform and stable) network state as a function of *IP3* with no stimulation (dots). Bumps contain a range of amplitudes and the maximum amplitude is shown. Bumps also grow in width with increasing *IP3* at approximately the same rate as they grow in amplitude (not shown). Bumps become possible with stimulation at approximately $IP3 = 0.45$, and are the globally attracting solution by approximately $IP3 = 0.77$. These simulations were carried out to 100 s, and in the region just above $IP3 = 0.77$, the (globally attracting) bump state developed more slowly than at higher levels of *IP3*.

the *network* relative to that of the Ca^{2+} subsystem standing alone.

We have a slightly different definition of conditional bistability than C-W, where the condition was an elevated network activity. Our conditional bistability requires neuronal firing plus a Ca^{2+} subsystem activated to excitability by IP3. When the Ca^{2+} subsystem by itself is excitable, neurons cannot lock into an elevated firing state (and thus form a bump) without the contribution from the Ca^{2+} subsystem, and the Ca^{2+} subsystem cannot lock into the elevated Ca^{2+} state without neuronal firing. Neither happens without the other. This is different from the previous case (above) where the Ca^{2+} subsystem itself was bistable. In that situation, neurons require elevated Ca^{2+} for elevated firing, but Ca^{2+} also can be elevated *without* neuronal firing. This may not be physiologically reasonable. We note also that bumps are not unique in shape in our hybrid model. We found previously that, in a restricted parameter regime, C-W supported bumps of varied width and amplitude (Fall et al., 2005). In our hybrid model this property is even more robust. Narrow stimuli can generate bumps which range from one neuron to an upper limit imposed by the shape of the connectivity kernel (results not shown). As with C-W, this property might depend strongly on background activity and other parameters, and we did not explore it in depth.

3.3. Bump Can be Smoother But is Still Robust to Noise

The nature and shape of the bump for our hybrid model differs from that in the original C-W model, as shown in the

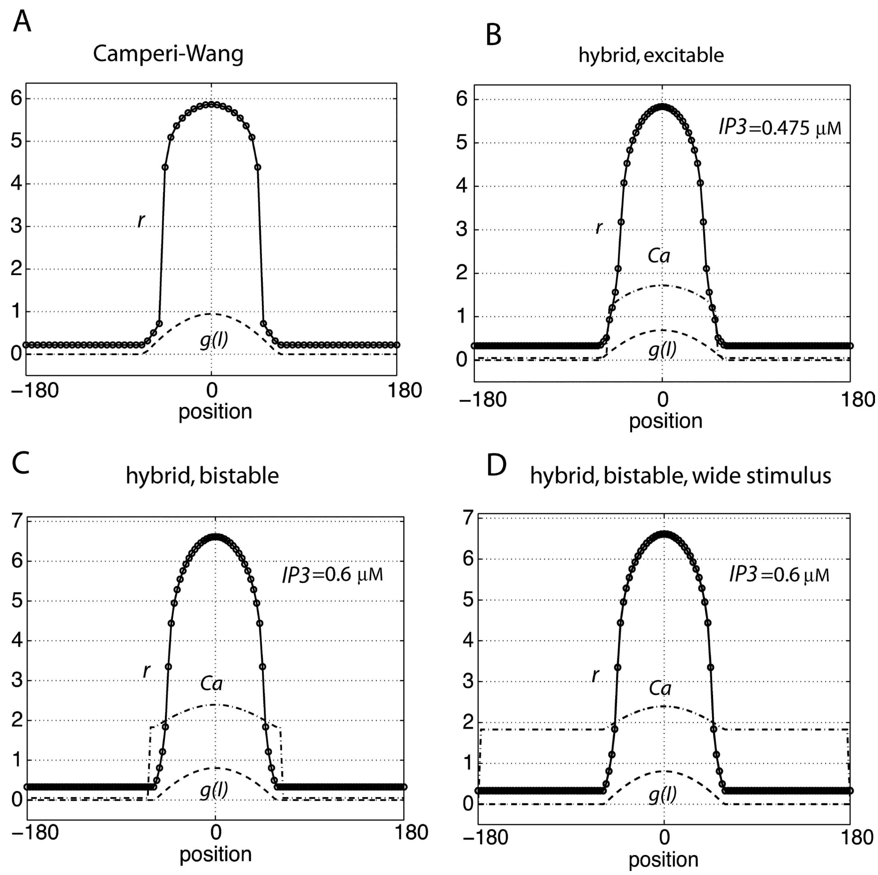

Fig. 5 **(A–D)** Profiles of stable bump states (10s) for (A) Camperi-Wang, (B) hybrid model tuned for Ca^{2+} subsystem excitability, (C) hybrid model tuned for Ca^{2+} subsystem bistability and (D) the same conditions as in (C) but with a wide, high amplitude stimulus ($I_{\text{cue}} = 5, p = 0.0001$). Firing rate profiles are shown in solid, with individual neurons indicated superimposed with circles. The value of the input function $g(I)$ is shown in dashes. Profiles for the Ca^{2+} subsystem are shown dash-dot in (B)–(D).

bump profiles of Fig. 5A–D. In these figures, the individual units are superimposed on the firing rate profile with circles. The firing rate in the C-W model, shown in Fig. 5A together with the input function $g(I)$, shows a sharp discontinuity in the bump profile due to bistability in the firing rate function (Camperi and Wang, 1998). Figure 5B shows the hybrid network tuned to excitability ($IP3 = 0.475\ \mu$M). Note that because the coupled system is conditionally bistable when the Ca^{2+} subsystem alone is excitable, Ca^{2+} is not elevated outside of the firing rate bump because the Ca^{2+} subsystem requires the influx of Ca^{2+} through J_{syn} due to synaptic drive in order to maintain the elevated state. Figure 5C shows the case for the bistable ($IP3 = 0.6\ \mu$M) version of the hybrid model. Note that the Ca^{2+} profile is slightly wider than the bump profile. The reason for this is that cells outside of the firing rate bump have their bistable Ca^{2+} subsystem activated to the high-Ca^{2+} state by the stimulus pulse (which is wider than the resulting bump). While these edge cells retain an elevated Ca^{2+} level, the lateral inhibition from the weight function constrains the firing rates and they do not demonstrate elevated firing. The uncoupling of elevated Ca^{2+} and neuronal activity in the bistable regime is further emphasized in Fig. 5D. Here a wide, high amplitude stimulus is presented to the network. Although neuronal firing is restricted by the connectivity again as in Fig. 5C, here the entire field shows elevated Ca^{2+}. Because the *r*-*Ca* coupling parameters for these simulations are effectively 1 and Ca^{2+} influx via J_{syn} depends directly on $g(I)$, the values for $g(I)$ shown in Fig. 5B–D show approximately how much Ca^{2+} contribution is a result of external input for the hybrid model.

In the hybrid model we have shifted the bistability from the firing rate function to the Ca^{2+} subsystem via coupling to the synaptic input. In contrast to C-W, firing rate dynamics are not discontinuous (as with an N-shaped f(r)). Because we use a smooth and monotonic firing rate function, neurons are not forced into an upper or lower firing rate branch and therefore have access to all values of r. Moreover the Ca^{2+} subsystem contributes to enhancing only a portion of the synaptic drive that leads to neuronal firing. Thus only a portion of the discontinuity in *Ca* is inherited by the firing rate r. This combination of a monotonic firing rate function and a bistable subsystem which contributes only a portion of the effective input allows for a bump of reduced discontinuity whether the Ca^{2+} subsystem is tuned for bistability or excitability.

In the original C-W formulation, the firing rate discontinuity between the bump state neurons and the lower state neurons was envisioned as diagnostic for intrinsic bistability in single cells. It was also shown to be a barrier over which neuronal firing rates would have to pass in order for the bump

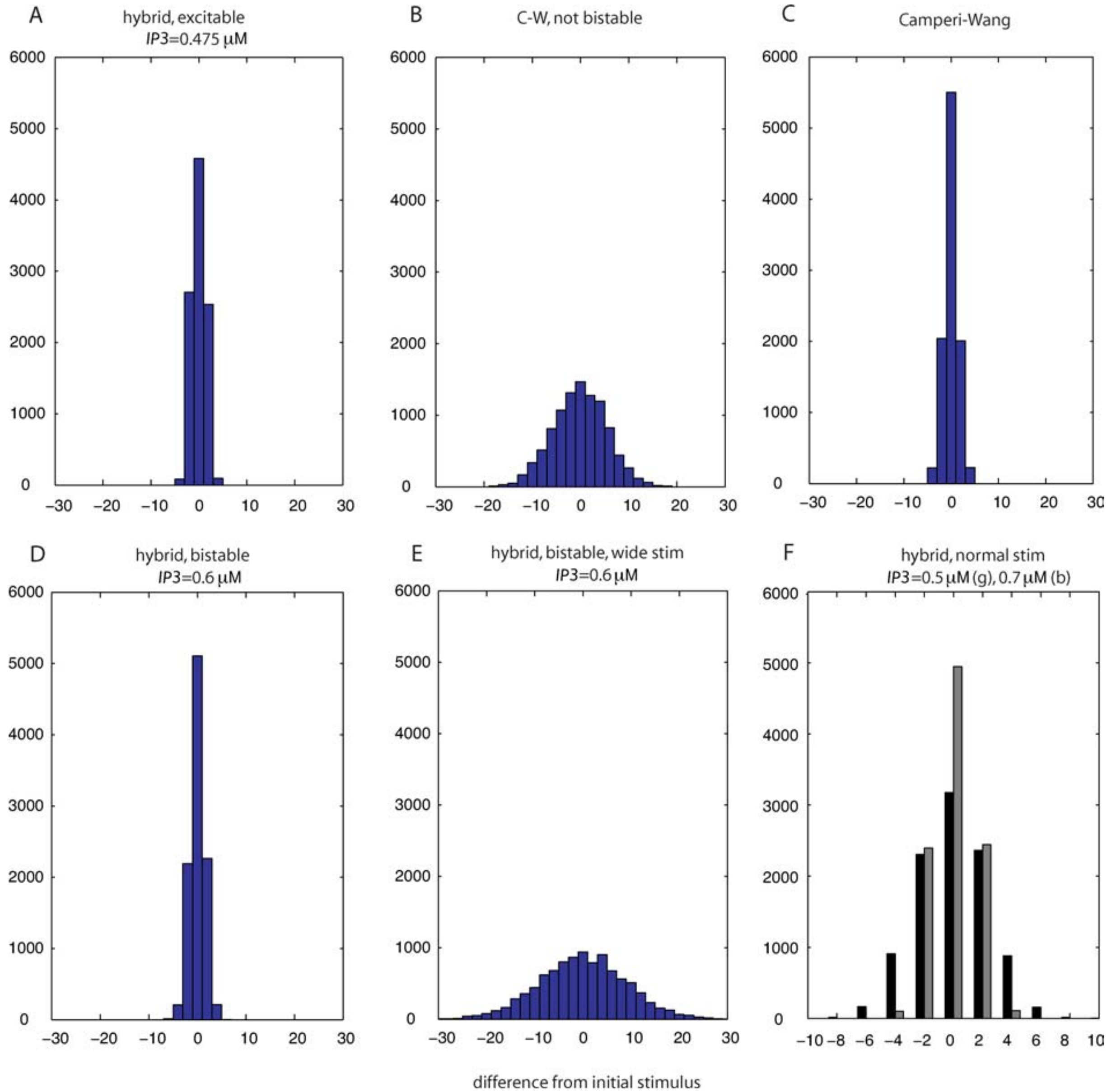

Fig. 6 Comparison of noise resistance between several different model variants. **(A):** Hybrid model tuned for excitability ($IP3 = 0.475\ \mu$M). **(B):** C-W model without bistability using modified piecewise linear input function (see Camperi and Wang (1998)). (C) The C-W model. (D) Hybird model tuned for bistability ($IP3 = 0.6\ \mu$M). (E) Hybrid model tuned for bistability ($IP3 = 0.6\ \mu$M), however a wide stimulus is given so that all neurons are in the upper Ca^{2+} state as in Fig. 5(D) and (F) Hybrid model with $IP3 = 0.5\ \mu$M (gray) and $IP3 = 0.7\ \mu$M (black), presented with normal stimulus on an expanded bottom axis. Shown are the distributions of the drift from initial position of population vectors (Camperi and Wang, 1998) 10 s after stimuli. Uniform white noise (0,1.5) was added to input I. Histograms represent 10,000 repetitions, and each model received the same sequences of pseudorandom numbers.

location to resist drift in the presence of noise. Because the bump resulting from the hybrid model is much smoother, we wondered if it would be resistant to noise. Camperi and Wang measured robustness to noise by tracking the population vector for the model (Camperi and Wang, 1998). Using this population vector, we computed drift from the initial stimulus after 10s between our model tuned for excitability, the C-W "linear" model without bistability (Camperi and Wang, 1998) and the standard C-W model with bistability. Figure 6(A–F) show histograms for 10,000 simulations with uniform white noise added to the input (I). Figure 6 shows that the hybrid model tuned for excitability (A) compares well with the original C-W model (C), both of which outperform the C-W model with no bistability (B) in resistance to drift. Surprisingly, increasing $IP3$ in the range of 0.425 μM to 0.6 μM did not significantly affect the final distribution after stochastic simulations (compare Fig. 6A with Fig. 6D), and the hybrid model tuned for bistability ($IP3 = 0.6\ \mu$M) also performs equally well when the typical stimulus is used. However when the bistable model is presented with a wide stimulus (Fig. 6E) so that the neurons are all in the high Ca^{2+} state (as in Fig. 5D), the network can no longer resist noise and actually performs slightly worse than the C-W model without bistability. Increasing *IP3* leads to an easier transition to the elevated Ca^{2+} state, and by $IP3 = 0.7\ \mu$M (Fig. 6F), which is still in the region of network bistability, the model presented with a normal stimulus begins to degrade (although it still outperforms the linear C-W variant). We note that the non-bistable C-W model also has a smooth bump profile (not shown) because the firing rate function is linear, and that maintenance of a bump requires changes to the connectivity profile (Camperi and Wang, 1998).

For our hybrid model, both the bistable and excitable Ca^{2+} subsystems result in a discontinuous Ca^{2+} profile at the edge of the bump (see Fig. 5B–C). Thus it is the Ca^{2+} subsystem which presents the energy barrier over which noise must overcome to transition neurons into the upper state and translate the bump profile. When the field of neurons is in the Ca^{2+} up state, as with the bistable hybrid model presented with a wide stimulus, it no longer resists noise perturbation. It is important to realize that noise introduced in the firing rate dynamics is buffered and thereby smoothed through the convolution term when it is felt by the Ca^{2+} subsystem. The resistance to noise in this formulation must surely depend on the sensitivity of the Ca^{2+} bistability and the coupling constants, which we did not explore in more detail.

4. Discussion

Here we have shown that a biologically plausible source of intrinsic bistability in individual neurons can lead to network bistability and working memory-like persistent bump activity in a simple hybrid model of working memory. We build on the work of Camperi and Wang (1988), but here intrinsic bistability in individual neurons was imparted using a Ca^{2+} subsystem which can be tuned for different dynamical behaviors. This Ca^{2+} subsystem is gated by the lipid-derived second messenger IP3, which is, in turn, produced via a G-protein coupled cascade. Many neuromodulators, including those thought to play a role in working memory and attention, have G-protein linked receptor variants. We envision that Ca^{2+} might up-regulate one or more of several currents that would lead to increased efficacy of synaptic input. Synaptic activity leads to increased cytosolic Ca^{2+} due to voltage gated Ca^{2+} channels and Ca^{2+} flux through synaptic channels.

The Ca^{2+} subsystem is tuned using the second messenger parameter *IP3*, and low levels of *IP3* did not admit stable bump solutions for the network. When we tuned the Ca^{2+} subsystem to be bistable, we found that the network easily produced working memory like bumps similar to those in the original C-W model. With strict bistability in the Ca^{2+} subsystem, it is possible for neurons to be in the high-Ca^{2+} state independent of firing. Because this did not seem physiological, we then tested whether an *excitable* Ca^{2+} subsystem could result in network bistability. An excitable Ca^{2+} subsystem may also result in a bistable network. Neurons must be both firing, thereby admitting external Ca^{2+}, and primed with IP3 in order for the neuron to lock into the high firing, high Ca^{2+} state. As is the case with C-W conditional bistability, only a subset of neurons on the edge of the active bump are actually bistable, and neurons firing at a higher rate at the bump center may have been pushed into the monostable-high Ca^{2+} regime. A prediction of this work is therefore that bistability of intracellular signaling in a single isolated cell may not necessarily be required for network bistability when recurrence alone is not sufficient. Instead, a more subtle amplification due to second messenger cascade excitability in single cells may permit network bistability. As excitable Ca^{2+} waves have been demonstrated in cortical neurons (Larkum et al., 2003), it may be useful to look at network activity under these same experimental conditions.

The connectivity structure and theme of bistability in this model is shared with the original C-W formalism. However, moving the bistability from the firing rate function to a second system which facilitates input to the neuron results in a model with important differences from the C-W work. Because of the bistable firing rate function in C-W, in which neurons are either on the upper or lower branch of the firing rate curve, there is a strong discontinuity in the shape of the working memory bump. Camperi and Wang suggest that this might be diagnostic of intrinsic bistability, such a claim might have to be limited to the case where the bistability is in the firing rate function. With the bistability not generated by the firing rate function, we are able to generate bumps that are less obviously discontinuous. Because the firing rate is coupled to the discontinuous Ca^{2+} subsystem, there must be a discontinuity in proportion to the contribution of Ca^{2+} to the firing rate. Despite a smoother-looking bump profile, our hybrid model is able to resist noise introduced in the input as well as the C-W model. Both models resist noise-induced drift better than the non-bistable C-W model, which also has a smooth profile.

Working memory implies bistability or multistability. In other words it requires a co-existence between a uniform "resting" state and a spatio-temporal activity state that persists following a brief transient input. In the case of bump-generating neural network models for working memory the maintenance of bump patterns is necessary but not sufficient for working memory performance. Such bump solutions for the network must co-exist with a stable uniform state (Fall et al., 2005). Here we have shown that there is a range of *IP3* for which a bump state co-exists with the stable uniform state and therefore is bistable, as required for working memory. As we found for C-W, a large region of parameter space in several models for persistent activity may guarantee existence of bump states but not network bistability of the type required for working memory (Fall et al., 2005). This property is mainly a function of the lateral inhibition connectivity kernel (Amari, 1977) which our model shares. At high levels of *IP3* the present model also has only the bump solution, and still higher levels of *IP3* result in a globally attracting bump state and a neural field with elevated Ca^{2+} in all neurons.

We investigate the plausibility of second messenger involvement with intrinsic cellular bistability. This is not the exclusive mechanism for intrinsic bistability: others have shown that interacting ionic membrane currents can generate bistability and plateau generating properties implicit in the C-W N-shaped firing function. While we have focused on the Ca^{2+} subsystem in this work, we regard it as a proxy for a diversity of intracellular signaling pathways that might be activated by neuromodulators. As other pathways are studied it is clear that some possess the autocatalytic activation and concentration-dependent inactivation which might lead to bistability and other interesting dynamical activity (Bhalla and Iyengar, 1999). It is not clear yet how the initiation and maintenance of persistent activity in this paradigm might depend on the relative timescales of a second messenger subsystem and neuronal integration, and this is work in progress.

Acknowledgments This work was supported by NIH MH 64611 to C.P.F. The authors also acknowledge the stimulating scientific environment and interactions at the NSF Mathematical Biosciences Institute, Ohio State University

References

Amari S (1977) Dynamics of pattern formation in lateral-inhibition type neural fields. Biol. Cybern. 27(2): 77–87.

Atri A, Amundson J, Clapham D, Sneyd J (1993) A single-pool model for intracellular calcium oscillations and waves in the Xenopus laevis oocyte. Biophysical Journal 65(4): 1727–1739.

Barbara JG (2002) IP3-dependent calcium-induced calcium release mediates bidirectional calcium waves in neurones: functional implications for synaptic plasticity. Biochim Biophys Acta 1600(1–2): 12–28.

Bhalla US, Iyengar R (1999) Emergent properties of networks of biological signaling pathways. Science 283(5400): 381–387.

Camperi M and Wang XJ (1998) A model of visuospatial working memory in prefrontal cortex: recurrent network and cellular bistability. J Comput Neurosci 5(4): 383–405.

De Young GW, Keizer J (1992) A single-pool inositol 1,4,5-trisphosphate-receptor-based model for agonist-stimulated oscillations in Ca^{2+} concentration. Proc Natl Acad Sci U S A 89(20): 9895–9899.

Durstewitz D, Seamans JK, Sejnowski TJ (2000) Neurocomputational models of working memory. Nat Neurosci 3(Suppl): 1184–1191.

Egorov AV, Hamam BN, Fransen E, Hasselmo ME, Alonso AA (2002) Graded persistent activity in entorhinal cortex neurons. Nature 420(6912): 173–178.

Ermentrount GB (2002) Simulating, Analyzing, and Animating Dynamical Systems: A Guide to XPPAUT for Researchers and Students. SIAM, New York.

Fall CP, Lewis TJ, Rinzel J (2005) Background activity dependent properties of a network model for working memory that incorporates cellular bistability. Biological Cybernetics.

Fall CP, Wagner JM, Loew LM, Nuccitelli R (2004) Cortically restricted production of IP3 leads to propagation of the fertilization Ca^{2+} wave along the cell surface in a model of the Xenopus egg. J. Theor. Biol. 231(4): 487–496.

Fransen E, Alonso AA, Hasselmo ME (2002) Simulations of the role of the muscarinic-activated calcium-sensitive nonspecific cation current INCM in entorhinal neuronal activity during delayed matching tasks. J. Neurosci. 22(3): 1081–1097.

Fuster JM (1988) The prefrontal cortex. Raven Press, New York.

Larkum ME, Watanabe S, Nakamura T, Lasser-Ross N, Ross WN (2003) Synaptically activated Ca^{2+} waves in layer 2/3 and layer 5 rat neocortical pyramidal neurons. J. Physiol. 549(Pt 2): 471–488. Epub 2003 Apr 11.

Li YX, Rinzel J (1994) Equations for InsP3 receptor-mediated $[Ca^{2+}]$i oscillations derived from a detailed kinetic model: a Hodgkin-Huxley like formalism. Journal of Theoretical Biology 166(4): 461–473.

Loewenstein Y, Sompolinsky H (2003) Temporal integration by calcium dynamics in a model neuron. Nat. Neurosci. 6(9): 961–967.

Nakamura T, Barbara JG, Nakamura K, Ross WN (1999) Synergistic release of Ca2+ from IP3-sensitive stores evoked by synaptic activation of mGluRs paired with backpropagating action potentials. Neuron 24(3): 727–737.

Nakamura T, Nakamura K, Lasser-Ross N, Barbara JG, Sandler VM, Ross WN (2000) Inositol 1,4,5-trisphosphate (IP3)-mediated Ca^{2+} release evoked by metabotropic agonists and backpropagating action potentials in hippocampal CA1 pyramidal neurons. J. Neurosci. 20(22): 8365–8376.

Seamans JK, Durstewitz D, Christie BR, Stevens CF, Sejnowski TJ (2001) Dopamine D1/D5 receptor modulation of excitatory synaptic inputs to layer V prefrontal cortex neurons. Proc Natl Acad Sci U S A 98(1): 301–306.

Seamans JK, Yang CR (2004) The principal features and mechanisms of dopamine modulation in the prefrontal cortex. Prog. Neurobiol. 74(1): 1–58.

Teramae J, Fukai T (2005) A Cellular Mechanism for Graded Persistent Activity in a Model Neuron and Its Implication in Working Memory. Journal of Computational Neuroscience 18(1): 105–121.

Wagner J, Fall CP, Hong F, Sims CE, Allbritton NL, Fontanilla RA, Moraru IILoew LM, Nuccitelli R (2004) A wave of IP3 production accompanies the fertilization Ca2+ wave in the egg of the fron Xenopus laevis: theoretical and experimental support. Cell Calcium. 35(5): 433–447.

Wang XJ (2001) Synaptic reverberation underlying mnemonic persistent activity. Trends Neurosci 24(8): 455–463.

Wilson HR, Cowan JD (1972) Excitatory and inhibitory interactions in localized populations of model neurons. Biophys. J. 12(1): 1–24.

Wilson HR, Cowan JD (1973) A mathematical theory of the functional dynamics of cortical and thalamic nervous tissue. Kybernetik 13(2): 55–80.

Yang CR, Seamans JK (1996) Dopamine D1 receptor actions in layers V-VI rat prefrontal cortex neurons in vitro: modulation of dendritic-somatic signal integration. J. Neurosci. 16(5): 1922–1935.